GeoFlow DNS: Non-rotational and rotational regimes of spherical gap flows

B. Futterer, C. Egbers

Dept. Aerodynamics and Fluid Mechanics,
Brandenburg University of Technology Cottbus, Germany

Topical Team
Geophysical Flow Simulation
Meeting
24-25 January 2008
BTU Cottbus, Germany

supported by: German Aerospace Center e.V. (DLR), grant number 50 WM 0122, European Space Agency (ESA), grant number AO99-049, ESA Topical Team, grant number 18950/05/NL/VJ

Outline

Research on convection in spherical shells, geophysically motivated

- central symmetry of buoyancy force field to simulate gravity fields
- parameter values very high (turbulence)
- rich variety of influences

  e.g. Coriolis force due to rotation, centrifugal force due to rapid rotation

  e.g. differential rotation vs. rigid body rotation
- physical properties of fluids

  e.g. low, moderate or high viscosity
- and the magnetic field?

GeoFlow experiment: spherical Rayleigh-Bénard conv.

- central force field by dielectrophoretic effect in microgravity environment
- non-rotating case
- rotational effects: transition to stabilizing effects by rapid rotation
- without magnetic effects

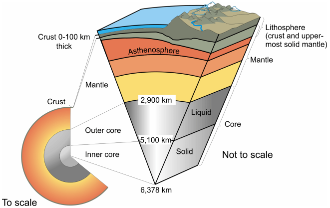

Earth's interior, Kious (1996)

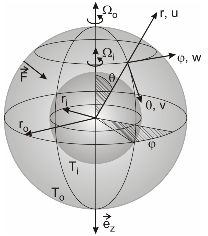

Rotating spherical model, inner sphere heated, with central force field

Equations for convection in rotating spherical shells with dielectric force field

$$\nabla \cdot \mathbf{U} = 0$$

$$Pr^{-1}\left[\frac{\partial \mathbf{U}}{\partial t} + (\mathbf{U}\cdot\nabla)\mathbf{U}\right] = -\nabla p + \nabla^2\mathbf{U} + \frac{Ra_{central}\; T}{\beta^2 r^5}\,\hat{\mathbf{e}}_r$$
$$-\sqrt{Ta}\,\hat{\mathbf{e}}_z \times \mathbf{U} + \widetilde{Ra}\; T\; r \sin\theta \hat{\mathbf{e}}_{eq}$$

$$\frac{\partial T}{\partial t} + \mathbf{U}\cdot\nabla T = \nabla^2 T$$

no-slip boundary conditions for velocity $\mathbf{U}$, temperature fixed $T(\eta) = 1$, $T(1) = 0$

Parameters

geometry	radius ratio	$\eta = \frac{r_i}{r_o}$
physical prop. of fluid	Prandtl number	$Pr = \frac{\nu}{\kappa}$
buoyancy (central force)	central Rayleigh number	$Ra_{central} = \frac{2\epsilon_0\epsilon_r\gamma}{\rho\nu\kappa}\; V_{\rm rms}^2\,\Delta T$
Coriolis force	Taylor number	$Ta = \left(\frac{2\Omega r_o^2}{\nu}\right)^2$
centrifugal force	additional Rayleigh number	$\widetilde{Ra} = \frac{\alpha\Delta T}{4}\; Ta\, Pr$

Spectral method

- decomposition of primary variables into poloidal and toroidal parts
- decomposition of these into Chebyshev polynomials and spherical harmonics
- solving equations for spectral coefficients

$$e(r,\theta,\varphi,t) = \sum_{m=0}^{M} \sum_{\ell=m'}^{L} \sum_{k=1}^{K} e_{k\ell m} T_{k-1}(x) P_\ell^{|m|}(\cos\theta) e^{im\phi}$$

- truncation with (K,L,M)=(30,60,20) resp. (30,60,60) for non-rotating case
- Hollerbach, R.: A spectral solution of the magneto-convection equations in spherical geometry, Int. J. Numer. Meth. Fluids 32 (2000), 773–797

Experimental constraints

				GeoFlow	outer core	mantle
gap width	$r_o - r_i[mm]$	13.5	$\rightarrow \eta$	0.5	0.37	0.55
viscosity	$\nu[m/s^2]$	$5 \cdot 10^{-6}$	$\rightarrow Pr$	64.64	0.1-1.0	∞, viscosity temp. depend. / layered
high voltage temperature	$V_{rms}[V]$ $\Delta T[K]$	10 ≤ 10	$\Big\}$ Ra	$\leq 1.4 \cdot 10^5$	$>10^{29}$	$10^6 - 10^8$
rotation rate	$n[Hz]$	≤ 2	$\rightarrow Ta$	$\leq 1.3 \cdot 10^7$	10^{30}	$<< 1$

Experimental Flow Plan

- set-up of high voltage field:
  set-up of artificial acceleration due to central force field
- non-rotating case:
  vary ΔT resp. Ra
- rotating case:
  set-up ΔT resp. Ra, superimpose n resp. Ta

Linear analysis for $Ta = 0$

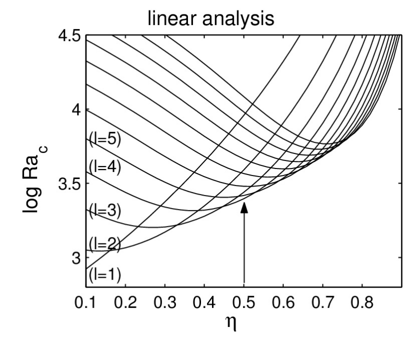

- critical Ra_{centr} for onset of convection independent on Pr
- larger $\eta \longrightarrow$ larger critical mode l

Source: Travnikov, V.; Egbers, C.; Hollerbach, R.: The GEOFLOW-experiment on ISS. Part II: Numerical simulation, Adv. Space Res. 32 (2003), 181–189

Travnikov V.: Thermische Konvektion im Kugelspalt unter radialem Kraftfeld, Dissertation, Cuvillier Verlag Göttingen, 2004

Linear analysis for $Ta \neq 0$

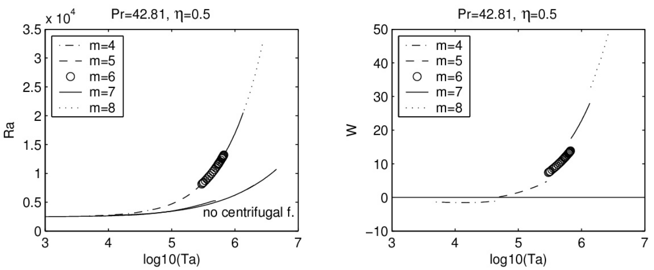

- shape of stability curves nearly independent on *Pr*
- instability due to Hopf bifurcation
- for large *Ta*: $Ra_{centr} \sim Ta^{2/3}$ [Roberts, P.H.: On the thermal instability of a rotating-fluid sphere containing heat sources, Philos. Trans. R. Soc. London 263 (1968), 93-117]
- drift velocity W changes sign (slows down or fastens rotation)

Source: Travnikov et al. (2003), Travnikov (2004)

Stability diagram and flow states

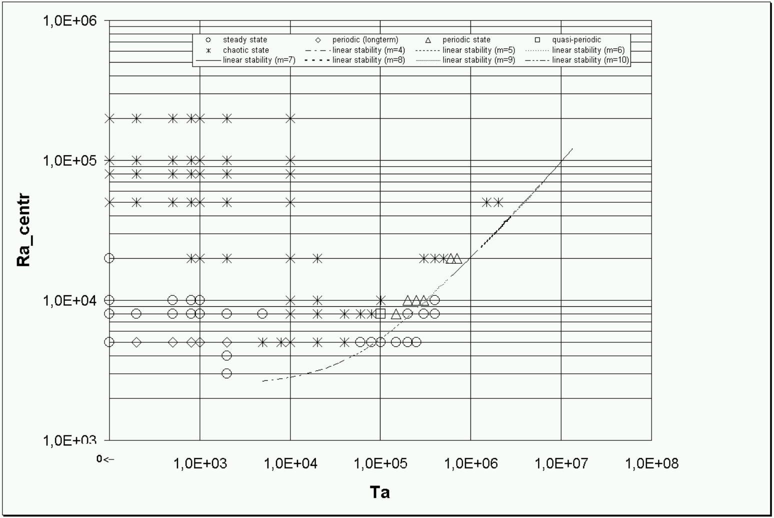

$\eta = 0.5$, $Pr = 64.64$, $Ta = 0$, Ra_{centr} increases stepwise: temperature field visualized on spherical surface in the gap, scaled to 100 %, cut view

$Ra_{centr} = 2 \cdot 10^3$ | $5 \cdot 10^3$ | $8 \cdot 10^3$

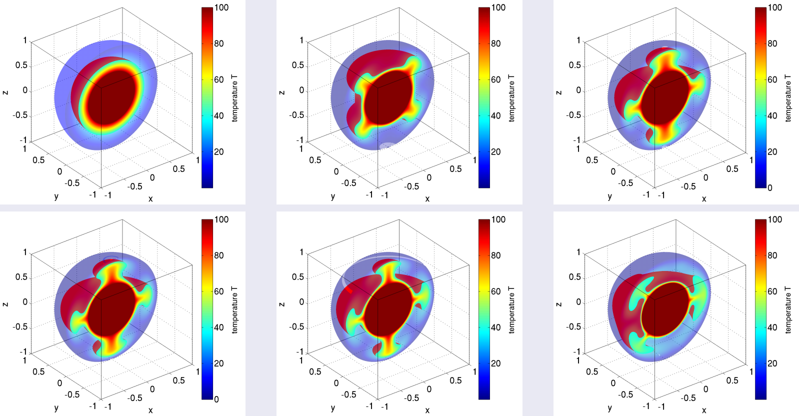

$1 \cdot 10^4$ | $2 \cdot 10^4$ | $5 \cdot 10^4$

$Ra_{centr} \leq 2 \cdot 10^4$ - steady fluid flow, $Ra_{centr} > 5 \cdot 10^4$ - time-dependent (irregular)

$\eta = 0.5$, $Pr = 64.64$, $Ta = 0$, Ra_{centr} increases stepwise: temperature field visualized on spherical surface in the gap, scaled to 100 %

$Ra_{centr} = 5 \cdot 10^3$ $\quad 8 \cdot 10^3$ $\quad 1 \cdot 10^4$

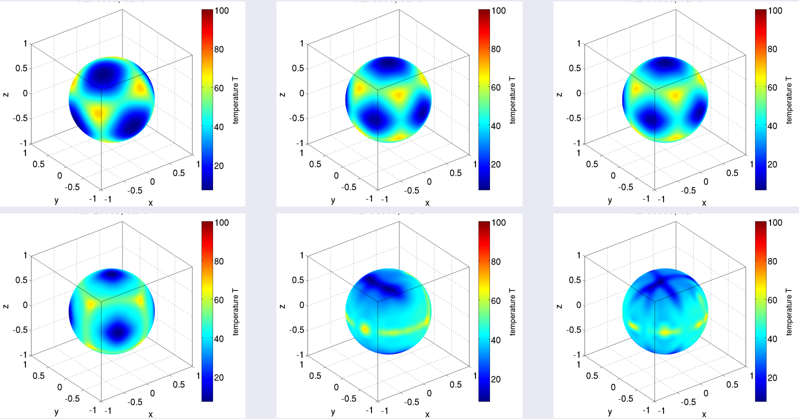

$2 \cdot 10^4$ $\quad 5 \cdot 10^4$ $\quad 8 \cdot 10^4$

$Ra_{centr} \leq 2 \cdot 10^4$ - steady fluid flow, $Ra_{centr} > 5 \cdot 10^4$ - time-dependent (irregular)

Stability diagram and flow states

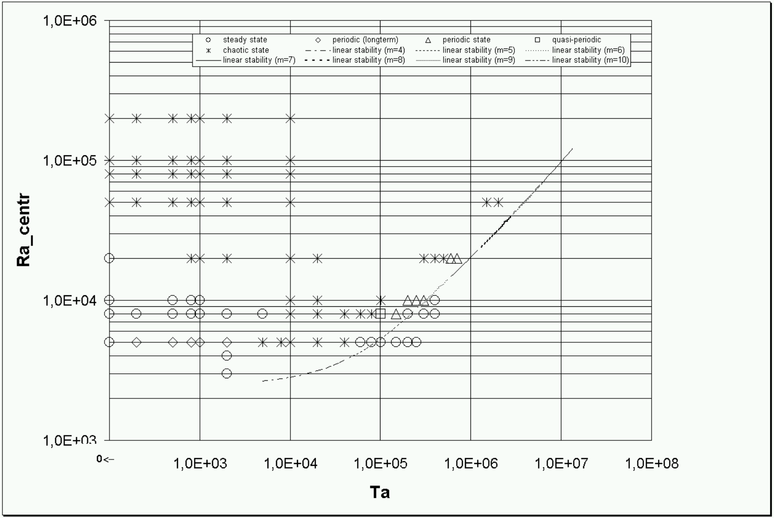

Ra_{centr} set, Ta increases: low rotation
temperature field visualized on spherical surface in the gap, scaled to 100 %

$Ra_{central}$	$Ta = 0$	$8 \cdot 10^2$	$2 \cdot 10^3$
$8 \cdot 10^3$	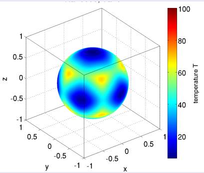 steady	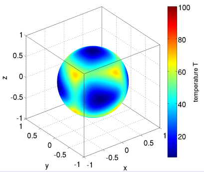 steady	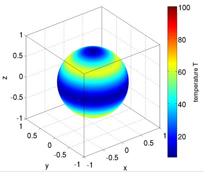 steady
$5 \cdot 10^3$	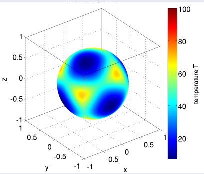 steady	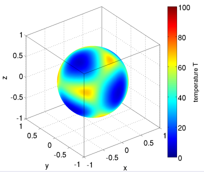 periodic longterm	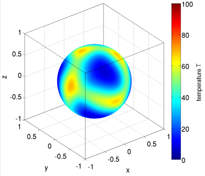 periodic longterm $n_{flow} = 0.000053\ Hz$ $n_{sphere} = 0.0244\ Hz$ drift prograd

Ra_{centr} set, Ta increases: intermediate rotation
temperature field visualized on spherical surface in the gap, scaled to 100 %

$Ra_{central}$ | $Ta = 1 \cdot 10^5$ | $1.5 \cdot 10^5$ | $2 \cdot 10^5$

$8 \cdot 10^3$

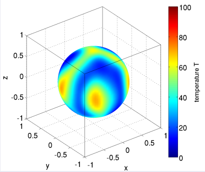

quasi-periodic
$n_{flow} = 250x0.0053\ Hz$
$n_{sphere} = 0.173\ Hz$
drift retrograd

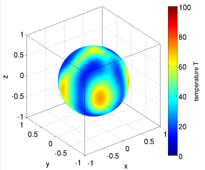

periodic
$n_{flow} = 0.0052\ Hz$
$n_{sphere} = 0.211\ Hz$
drift retrograd

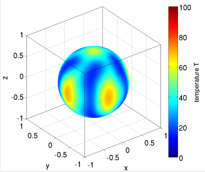

steady

$5 \cdot 10^3$

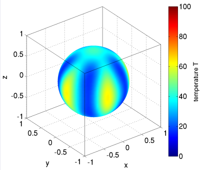

steady

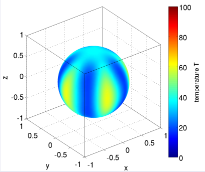

steady

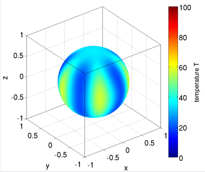

steady

Summary

- non-rotating case
  - stability analysis gives onset of convection
  - DNS shows transition from steady to irregular flow
  - influence of initial conditions shown
  - analyses of stable states with path following methods $\longrightarrow$ Bergemann et al. (2007)
  - timeseries analysis with nonlinear methods
- rotating case
  - stability analysis shows influence of centrifugal forces
  - change of sign for drift velocity
  - DNS shows complex pattern drift with different sign
  - request for path following methods for steady states, especially in low rotation regime
  - further timeseries analysis

Outlook

- use of results for interpretation of interferograms
- discussion and interpretation